Self-consistent, Lithospheric Stress-modulated Growth of Large Volcanic Edifices on Venus: Scenarios for Creation of Conical and Domical Edifices, and Several Different Topographic Groups of Coronae. P. J. McGovern[1] and J. Buz[2], [1]Lunar and Planetary Institute, USRA (3600 Bay Area Blvd., Houston, TX, 77058; mcgovern@lpi.usra.edu), [2]Dept. of Physics and Astronomy, Northern Arizona University (Flagstaff, AZ 86011).

Introduction: The geomorphic term "corona", formally and simply defined as "an ovoid feature" by the International Astronomical Union [1], has accumulated a dense carapace of meaning as applied to a class of features on the planet Venus characterized by annular tectonics and/or topography [e.g., 2,3]. In the decades since the completion of NASA's Magellan mission, the conventional wisdom has held that corona formation results from deformation of the lithosphere from mantle convective tractions and uplift from viscous flow of upwelling diapirs [4,5]. Despite evidence for a continuum of volcanic processes spanning the range of "conventional" volcanic edifice to corona, either simply by observation of copious volcanism or via identification of "hybrid volcano-corona" features like Atai Mons [6], a role for volcanic edifice construction in corona formation has been relatively ignored (see [7,8] for possible exceptions).

Favored corona models have invoked basal uplift, viscous deformation of substrate, convection, even subduction [4-10]. An alternative explanation is through volcanic edifice construction, building off suggestions that lithosphere thickness T_e exerts control on edifice shape via flexural wavelength [11]. Buz and McGovern [12] demonstrated that the ratio of magma flux rate dm/dt to the mantle viscous relaxation time τ_M played a role, such that when this ratio was small (as expected for most large volcanoes), a variety of edifice shapes including annular (i.e., corona-like) could be produced given favorable T_e values.

Methods: We model self-consistent growth of a volcanic edifice on Venus by calculating the interaction of the lithospheric stress state generated by lithospheric flexure and favored magma ascent pathways [11,12]. In each model, a characteristic magma source radius (r_m) and central height (h_m) are defined. Magma distribution is then subdivided into a number, n_{inc}, of equal height increments (n_{inc} = 20 here; such a high n_{inc} value corresponds to the low $(dm/dt)/\tau_M$ ratio case described above). For a given stress state, magma ascent at a given location depends on two criteria [11, 12]: favorable horizontal normal stress orientations (horizontal extension) and gradients (extension increasing upward). Our model evaluates these criteria as functions of radius r at a discrete set of points, with allowances for favorable stress (e.g., regional) and stress gradient (e.g., magma buoyancy) terms that offset adverse values. Then the magma height for the current increment is assigned to points in r where both ascent criteria are satisfied,; at points where one or both criteria are violated, the magma is diverted to the closest value of r where both ascent criteria are satisfied. Then the material is distributed according to an algorithm described below, simulating lateral motion of flowing lava. Then a new flexural stress state is calculated for a load comprising the load from previous increments plus the just-calculated load distribution for the new increment, and the cycle is repeated n_{inc} times.

Lava distribution. We implement a diffusion algorithm originally applied to diffusive transport of sediments over seamounts [13] to distribute magma from its eruption sites over the pre-existing surface topography. Our intent is not to model the dynamics of a particular lava flow or group thereof in a rigorous way, but rather to create a means of smoothly distributing lava at a potentially irregular distribution of eruption sites in a way that reflects the natural driving forces for flow (i.e., downward flow over pre-existing topography) and conservation of mass. The distributed lava and flexural response thereto then constitutes the basal topography for the subsequent load increment.

Results and Discussion: We examined the effect of lithospheric thickness T_e and incremental edifice growth on edifice shapes over a range of conditions appropriate to Venus. We re-confirmed the general findings of [11,12] that elastic lithosphere thickness exerts a strong influence on the shape of self-consistently grown volcanic edifices (Figure 1). At the completion of formation of an edifice emplaced on a lithosphere with low elastic thickness (T_e = 10 km, blue line in Fig. 1), a central domical high and annular distal high ("rim") is evident, corresponding to topographic group 3b "Rim surrounding interior dome" of [4]. As T_e is increased to 20 km & 30 km, the central dome disappears but the central region is still elevated and the distal rim is maintained, leaving a profile resembling class 3a "Rim surrounding interior high". As T_e is increased further, the rim disappears leaving a domical and eventually somewhat conical edifice at the T_e = 60 km (Fig. 1). We note that the diffusive flow algorithm tends to smooth out the initial shape of the underlying distribution of magma (conical in all cases shown here), resulting in substantially fewer strictly conical edifices than were found in [12].

In addition to considering final edifice shapes (Fig. 1), tracking the shape of a single volcano as a function of load increment reveals important new insights into corona formation. For an edifice with T_e = 20 km (Fig. 2), the initial load increment creates a dome (not shown) that more or less reflects the subsurface magma distribution. After five increments (blue line in Figure 1), lithospheric stresses shut off central eruption and favor distal eruption to create a rim, with a center low enough to suggest a transition from topographic groups 3a to 4 ("rim surrounding depression") [4]. Further, at 10 and 15 increments the center surface is actually below the zero level(!), a consequence of the mass of the rim load operating on moderate-thickness lithosphere with a flexural wavelength long enough to cause depression of the central region, as opposed to a "form-fitting" response at low-thickness lithosphere which would have created an annular flexure beneath the annular surface load. This finding negates assertions that a group 4-type profile requires some sort of mantle convective or other fluid-driven process to form. After emplacement of 20 increments, flexural response to the distal load has 1) re-opened central magma ascent, allowing creation of a central dome, and 2) created a deep outboard trough; collectively, these produce a group 5 "Outer rise, trough, rim, inner high" profile [4]. These results demonstrate that a wide range of corona shapes can be produced by a self-consistent constructional model for volcanic edifice growth, thereby expanding the range of conditions that can produce corona morphologies [14].

These models make specific tectonic and stratigraphic predictions that can be tested through the observed geologic record to distinguish coronae formed by a constructional mechanism (under the given model conditions) from those formed by subsurface-driven deformation. These include exposures of older terrain on the inner-facing flank of annular ridges (e.g., Fig. 3, yellow and green lines above 0 km height), and young flows on the outer flank and at the center within the ridge if central magma ascent is reactivated.

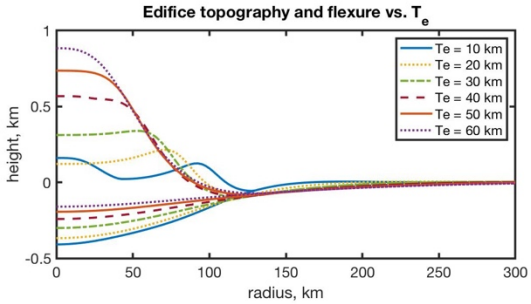

Figure 1. Final volcanic edifice topography and lithospheric flexural profile vs. radius, for models lithosphere thickness T_e values ranging from 10 to 60 km. Initial magma source distribution is conical with radius 50 km, height 5 km, and applied in 20 equal-volume increments. Vertical exaggeration = 100 in all Figures.

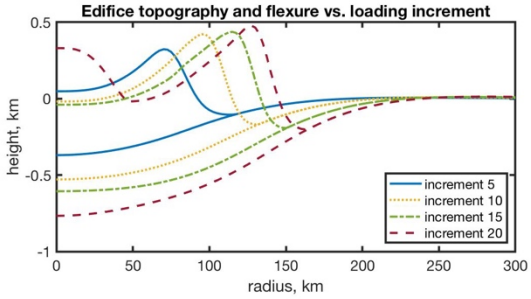

Figure 2. Volcanic edifice topography and lithospheric flexural profile after emplacement of 5, 10, 15, and 20 load increments, for model with initial conical magma source distribution of 100 km radius and 5 km height and T_e = 15 km.

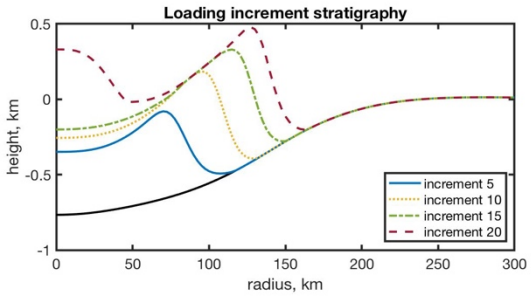

Figure 3. Volcanic stratigraphy of buried former edifice surfaces for increments 5, 10, and 15, and final topography of increment 20, for the model in Figure 2.

References: [1] International Astronmical Union (2018) https://planetarynames.wr.usgs.gov/ . [2] Pronin A. A. and Stofan E. R. (1990) *Icarus* **87**, 452–474. [3] Stofan E. R. et al. (1992) *J. Geophys. Res. Planets* **97**, 13347–13378. [4] Smrekar S. E. and Stofan E. R., *Science, 277*, 1289-1294. [5] Koch D. M. and Manga M. (1996) *Geophys. Res. Lett.* **23**, 225–228. [6] Grindrod P. M. et al., (2004) *J. Geol. Soc. Lond.*. **163**, 265-275. [7] Janes D. M. et al. (1992) *J. Geophys. Res. Planets* **97**, 16055–16067. [8] Squyres S. W. et al. (1992) *J. Geophys. Res. Planets* **97**, 13611–13634. [9] Stefanick M. and Jurdy D. M. (1996) *J. Geophys. Res. Planets* **101**, 4637–4643. [10] Sandwell D. T. and Schubert G. (1992) *Science,* **257**, 766. [11] McGovern P. J. et al. (2013) *J. Geophys. Res. Planets* **118**, 2423–2437. [12] Buz J. and McGovern P. J. (2010) *Lunar and Planetary Science Conference*, p. 1482. [13] Webb H. F. and Jordan T. H. (2001) *J. Geophys. Res. Solid Earth* **106**, 30451–30473. [14] Hoogenboom T. et al. (2005) *J. Geophys. Res. Planets* **110**, DOI 10.1029/2004JE002394.